MIT Open Access Articles

Characterization and modification of enzymes in the 2-ketoisovalerate biosynthesis pathway of Ralstonia eutropha H16

Massachusetts Institute of Technology

Title: Characterization and Modification of Enzymes in the 2-Ketoisovalerate Biosynthesis

Pathway of *Ralstonia eutropha* H16

Jingnan Lu[1], Christopher J. Brigham[2], Jens K. Plassmeier[3], Anthony J. Sinskey[3, 4, 5]*

Department of Chemistry[1], Massachusetts Institute of Technology, 77 Massachusetts Avenue,

Cambridge, Massachusetts 02139, USA

Department of Bioengineering[2], University of Massachusetts Dartmouth, 285 Old Westport

Road, North Dartmouth, MA 02747, USA

Department of Biology[3], Division of Health Sciences and Technology[4], Engineering Systems

Division[5], Massachusetts Institute of Technology, 77 Massachusetts Avenue, Cambridge,

Massachusetts 02139, USA

* Corresponding author. Mailing address: Bldg. 68-370, Department of Biology,

Massachusetts Institute of Technology, 77 Massachusetts Ave., Cambridge, MA 02139, USA.

Phone: (617) 253-6721. Fax: (617) 253-8550. E-mail: asinskey@mit.edu

ABSTRACT

2-ketoisovalerate is an important cellular intermediate for the synthesis of branched-chain amino acids, as well as other important molecules, such as pantothenate, coenzyme A, and glucosinolate. This ketoacid can also serve as a precursor molecule for the production of biofuels, pharmaceutical agents, and flavor agents in engineered organisms, such as the betaproteobacterium *Ralstonia eutropha*. The biosynthesis of 2-ketoisovalerate from pyruvate is carried out by three enzymes: acetohydroxyacid synthase (AHAS, encoded by *ilvBH*), acetohydroxyacid isomeroreductase (AHAIR, encoded by *ilvC*), and dihydroxyacid dehydratase (DHAD, encoded by *ilvD*). In this study, enzymatic activities and kinetic parameters were determined for each of the three *R. eutropha* enzymes as heterologously-purified proteins. AHAS, which serves as a gate-keeper for the biosynthesis of all three branched-chain amino acids, demonstrated the tightest regulation through feedback inhibition by L-valine (IC_{50} = 1.2 mM), L-isoleucine (IC_{50} = 2.3 mM), and L-leucine (IC_{50} = 5.4 mM). Intermediates in the valine biosynthesis pathway also exhibit feedback-inhibitory control of the AHAS enzyme. In addition, AHAS has a very weak affinity for pyruvate (K_M = 10.5 μM) and is highly selective towards 2-ketobutyrate (R = 140) as a second substrate. AHAIR and DHAD are also inhibited by the branched-chain amino acids, although to a lesser extent when compared to AHAS. Experimental evolution and rational site-directed mutagenesis revealed mutants of the regulatory subunit of AHAS (IlvH) (N11S, T34I, A36V, T104S, N11F, G14E, and N29H), which, when reconstituted with wild type IlvB, lead to AHAS having reduced valine, leucine, and isoleucine sensitivity. Study of the kinetics and inhibition mechanisms of *R. eutropha* AHAS, AHAIR, and DHAD has shed light on interactions between these enzymes and the products they produce; therefore can be used to engineer *R. eutropha* strains with optimal production of 2-ketoisovalerate for value-added materials.

INTRODUCTION

The metabolically versatile proteobacterium *Ralstonia eutropha*, also known as *Cupriavidus necator*, is a tremendously important organism in biotechnological research and development. *R. eutropha* is notably capable of utilizing numerous simple and complex carbon sources derived from common waste streams, including carbon dioxide, oils and fats, and mixed organic acids (Bowien and Kusian 2002; Cramm 2009; Kohlmann et al. 2011; Pohlmann et al. 2006; Schwartz et al. 2009). Wild type *R. eutropha* stores carbon and energy in the form of polyhydroxyalkanoate (PHA), a type of biodegradable plastic, under unbalanced nutrient stress high in carbon (Brigham et al. 2012; Cramm 2009; Ishizaki et al. 2001; Pohlmann et al. 2006). Elimination of the enzymes responsible for the production of PHA in *R. eutropha* resulted in a strain capable of secreting a large amount of pyruvate and stored more NADH reducing equivalent compared to the wild type (Lu et al. 2012; Raberg et al. 2014). Additionally, other reduced metabolites such as 2,3-butanediol, ethanol, lactate, butanol, and 3-hydroxybutyrate are also secreted (Vollbrecht et al. 1978; Vollbrecht and Schlegel 1978; Vollbrecht and Schlegel 1979). There is a growing interest in repurposing these secreted pyruvate and extra energy compounds in these PHA-negative strains into value-added chemicals, such as biofuels, pharmaceutical precursors, and flavoring agents (Brigham et al. 2012). Recent accomplishments among many others in engineering PHA-negative strains of *R. eutropha* include the production of biofuels from branched-chain amino acid (BCAA) and PHA production precursors (Brigham et al. 2013; Brigham et al. 2012; Grousseau et al. 2014; Lan and Liao 2013; Li and Liao 2014; Li et al. 2012; Lu et al. 2012).

The production of isobutanol, a next-generation drop-in biofuel, was achieved through the BCAA biosynthesis pathway. The key precursor 2-ketoisovalerate, an intermediate of the valine biosynthesis pathway synthesized from pyruvate, can be decarboxylated to form isobutyaldehyde and subsequently reduced into isobutanol. Recently, numerous groups were able to redirect pyruvate into isobutanol in engineered *R. eutropha*; however, the production

3

titer remains relatively low as compared to other engineered organisms (Brigham et al. 2013; Li et al. 2012; Lu et al. 2012). The main challenge faced has been the lack of understanding of the interaction and regulation of enzymes that produce the key precursor molecule, 2-ketoisovalerate, in *R. eutropha* (Lu et al. 2012). Utilization of the well-studied biosynthesis enzyme AHAS from *Bacillus subtilis* was reported to be toxic to *R. eutropha* cells, thus precluding their use in production strain engineering (Li and Liao 2014; Li et al. 2012).

Acetohydroxyacid synthase (AHAS) catalyzes the most important step in the 2-ketoisovalerate biosynthesis pathway, since the reactions it catalyzes are irreversible and are the first committed steps towards the synthesis of all three BCAAs (Figure 1). AHAS is capable of synthesizing 2-acetolactate, a precursor of valine and leucine from two molecules of pyruvate, in addition to 2-aceto-2-hydroxybutyrate, a precursor of isoleucine from pyruvate and 2-ketobutyrate. A bifunctional AHAS catalyzes both of the above-mentioned reactions in most organisms, whereas in a few organisms, two separate enzymes catalyze these reactions (Chipman et al. 1998; McCourt and Duggleby 2006). *R. eutropha* AHAS enzyme consists of two subunits, IlvB and IlvH, encoded by genes in the operon *ilvBHC* (locus tags H16_A1035 and H16_A1036). To date, there is no definitive structural information on AHAS, although individual subunits have been crystallized separately from *Escherichia coli* (Chipman et al. 1998; Kaplun et al. 2006; McCourt and Duggleby 2006; Park and Lee 2010; Petkowski et al. 2007). Studies of AHAS from *E. coli*, *Corynebacterium glutamicum*, *B. subtilis*, *Lactococcus lactis,* and others have led to the hypothesis that catalysis occurs at the IlvB homodimer interface and IlvH is required for catalysis, but serves a regulatory role. The expression of *ilvBH* is controlled by the amount of charged-tRNA[BCAAs] available in the cell. High levels of charged-tRNA[BCAAs] repress the transcription of *ilvBH*. Furthermore, AHAS activity is controlled allosterically at the activity level by its regulatory subunit IlvH, through binding of BCAA at the homodimer interface (Barak and Chipman 2012; Chipman et al. 1998; Eggeling

et al. 1987; Eoyang and Silverman 1986; McCourt and Duggleby 2006; Vinogradov et al. 2006).

E. coli has three extensively-studied AHAS isozymes, each with a different substrate specificity and regulation mechanism. The sequence of *E. coli* AHAS isozyme II differs from the other two AHASs, and its regulatory subunit is insensitive to direct feedback inhibition by valine (Eoyang and Silverman 1986; Park and Lee 2010; Steinmetz et al., 2010; Vinogradov et al. 2006; Vyazmensky et al. 2009; Vyazmensky et al. 1996). *R. eutropha* AHAS shares the greatest sequence similarity with *E. coli* AHAS isozyme I (52%); therefore, it could also be subject to allosteric feedback inhibition by the pathway intermediates 2,3-dihydroxy-isovalerate and 2-ketoisovalerate, in addition to the end products valine, leucine, and isoleucine. Thus, understanding and minimizing allosteric inhibition by products and intermediates are essential to optimize the production of 2-ketoisovalerate in *R. eutropha*.

In the case of *R. eutropha*, AHAS catalyzes both the formation of 2-acetolactate and 2-aceto-2-hydroxybutyrate (Figure 1). The substrate selectivity ratio (R) towards 2-ketobutyrate as the second substrate over pyruvate can be calculated by the following equation:

$$R = \frac{[AHB]}{[2KB]} \Big/ \frac{[AL]}{[P]} \quad \text{(Equation 1)}$$

where AHB, 2KB, AL, and P represent 2-aceto-2-hydroxybutyrate, 2-ketobutyrate, 2-acetolactate, and pyruvate respectively (Barak et al. 1987; Gollop et al. 1990). There is a competition between pyruvate and 2-ketobutyrate for an active 2-hydroxyethyl-TPP carbanion/enamine intermediate formed irreversibly after the addition and decarboxylation of the first pyruvate moiety to the enzyme (Bar-Ilan et al. 2001; Chipman et al. 2005; Engel et al. 2004; Steinmetz et al. 2010; Tittmann et al. 2004; Vyazmensky et al. 2011). R values for *E. coli* AHAS isozymes I, II, and III are respectively 1, 185, and 53. These ratios, besides that of isozyme I, strongly favor the formation of 2-aceto-2-hydroxybutyrate over 2-acetolactate (Barak et al. 1987).

Acetohydroxyacid isomeroreductase (AHAIR), encoded by *ilvC* (locus tags H16_A1037) within the operon *ilvBHC* in *R. eutropha*, catalyzes the formation of 2,3-dihdroxyisovalerate from 2-acetolactate, in addition to the formation of 2,3-dihydroxy-3-methylvalerate from 2-aceto-2-hydroxybutyrate. Unlike AHAS, AHAIR has similar substrate preference towards both substrates. AHAIR requires NADPH and a divalent metal ion, in most cases Mg^{2+}, for catalysis. The metal cofactor is involved in the alkyl migration isomerization step, whereas NADPH is the electron donor for the reduction step. A unique feature of its reaction mechanism is that it simultaneously catalyzes both an isomerization and a reduction reaction. Mutations in active site residues that abolished the reductase activity also eliminated the isomerization reaction, suggesting that isomerization and reduction are coupled without any detectable intermediate (Chunduru et al. 1989; Harper et al. 1984; Schomburg and Stephan 1995).

Dihydroxyacid dehydratase (DHAD) catalyzes the formation of ketoacids from the products of AHAIR. In most organisms, DHAD encoded by *ilvD* is found in the BCAA biosynthesis operon *ilvBHCD* (Eggeling et al. 1987; Krause et al. 2010; Leyval et al. 2003). However, the *R. eutropha ilvD* (locus tag H16_A2987) gene is not found in the operon, but elsewhere on chromosome I. The mechanism of action is not yet elucidated, but was hypothesized to involve the dehydration of vicinal diols to ketoacids via an enol intermediate. *E. coli*'s oxygen-sensitive DHAD contains a $[4Fe-4S]^{2+}$ cluster. The reaction mechanism is proposed to be similar to that of aconitase in the TCA cycle, which also involves a FeS cluster (Flint and Emptage 1988; Flint et al. 1993; Leyval et al. 2003). As shown in Figure 1, the combined activities of AHAS, AHAIR, and DHAD convert pyruvate into the key intermediate 2-ketoisovalerate.

The specific activity, substrate specificity, and feedback inhibition of *R. eutropha* AHAS, AHAIR, and DHAD have not been previously studied. In order to better understand

the catalysis of these enzymes and to minimize allosteric inhibition, AHAS, AHAIR, and DHAD were isolated as pure enzymes and evaluated in this study.

MATERIALS AND METHODS

Chemicals, bacterial strains, and plasmids

Unless indicated otherwise, chemicals used in this study were purchased from Sigma-Aldrich. Strains and plasmids used were listed in Table 1. Mutant strains were all derived from wild type *R. eutropha* H16 (ATCC 17699). Primers used in the construction of plasmids and strains were listed in Online Resource 1.

Growth media and cultivation conditions

As described previously by Lu et al. 2012, *R. eutropha* strains were cultivated aerobically in rich and minimal media with 2% (w/v) fructose at 30°C. Gentamicin at 10 μg/mL final concentration was added to all *R. eutropha* cultures (Walde 1962). *E. coli* cultures were grown in lysogeny broth (LB) at 30°C with the addition of 100 μg/mL amplicillin and 34 μg/mL chloramphenicol (Lu et al. 2013; Lu et al.2012).

R. eutropha growth experiments with different concentrations of 2-ketoisovalerate or valine were conducted by supplementing minimal media with 0 to 0.5% (w/v) 3-methyl-2-oxobutanoic acid sodium salt or 0 to 1 mM L-valine, respectively. Fructose, antibiotics, 3-methyl-2-oxobutanoic acid sodium salt, and L-valine, were all filter sterilized while the rest of the medium components were sterilized by autoclaving.

Experimental evolution of L-valine

Wild type *R. eutropha* H16 cells were cultivated in minimal media until OD_{600} reached 3.0. Aliquots of the culture were then transferred to fresh minimal media supplemented with L-valine at concentrations of 0.1 mM to reach initial OD_{600} of 0.1. The cultures were

sequentially transferred to inoculate fresh minimal media with increasing concentration of L-valine when they reached OD_{600} of 3.0. Over the 60-day time course, L-valine concentration was increased from 0.1 mM to 10 mM in the growth media.

In order to detect mutations evolved that could contribute to valine insensitivity by AHAS, *ilvB* and *ilvH* genes in addition to 100 base pairs (bp) of DNA sequence upstream and downstream of *ilvBH* were amplified by PCR, sequenced, and compared between wild type and mutant (Re2452) strains.

Plasmid and strain construction

Standard molecular biology techniques were utilized for all DNA manipulations (Sambrook et al. 2001). Amplification of DNA sequence was achieved using Phusion DNA polymerase (New England Biolabs, Ipswich, MA). QIAquick gel extraction kit (Qiagen, Valencia, CA) and QIAprep spin miniprep kit (Qiagen, Valencia, CA) were used for gel purifications of all DNA products and plasmid extractions respectively. Restriction enzymes used in this study were from New England Biolabs (Ipswich, MA).

Construction of plasmids for the heterologous overexpression of BCAA enzymes was first carried out by amplifying genes *ilvB*, *ilvH*, *ilvC*, and *ilvD* that encode IlvB, IlvH, IlvC, and IlvD, respectively, from the genome of wild type *R. eutropha* H16. The PCR amplifications with primers listed in Online Resource 1 added a *Nde*I site to the 5' end of each gene and a *Bam*HI site to the 3' end. The PCR fragments were purified on 0.8% agarose gel. Both PCR fragments and expression vector pET15b were digested with *Nde*I and *Bam*HI, and then ligated together and transformed into high efficiency *E. coli* DH10-beta competent cells (New England Biolabs, Ipswich, MA) to create the expression plasmid. Each expression plasmid contained a gene encoding N-terminal six-His-tagged version of each enzyme. Lastly, the plasmids were transformed into *E. coli* strain Tuner(DE3) for inducible protein expression.

The Tuner(DE3) strain also contained an additional plasmid, pRARE that allows for translation of protein with rare-codons.

Plasmid for markerless deletion of *ilvH* was constructed by first amplifying approximately 500 bp of DNA sequence upstream and downstream of *ilvH* using primers with identical sequence overlap at the end (Online Resource 1). Overlap PCR using these primers resulted in a DNA fragment of approximately 1,000 bp in length that contained both the upstream and downstream region of *ilvH*. The DNA fragment and plasmid pJV7 (Budde et al. 2010) (Table 1) were digested with the restriction enzymes *Xba*I and *Bam*HI, and then ligated together with the *ilvH* deletion fragment to form the deletion plasmid. The resulting plasmid was verified in *E. coli* DH10-beta competent cells before being transformed into *E. coli* S17-1 (Simon et al. 1983) , which was used as a donor for the conjugative transfer of mobilizable plasmids. A standard mating and gene deletion procedure was performed as described previously (Quandt and Hynes 1993; Slater et al. 1998; York et al. 2001). Deletion strains were screened by diagnostic PCR with pairs of internal and external primer sets (Online Resource 1).

Site-directed mutagenesis was achieved by overlap extension PCR method using primers listed in Online Resource 1 using plasmid pJL14 as the template DNA. This method allowed for single nucleotide mutations with site specificity.

Purification of His-tagged proteins and removal of the His-tag

R. eutropha enzymes in the 2-ketoisovalerate production pathway were expressed in *E. coli* (Table 1) and purified. *E. coli* Tuner(DE3) with pRARE and BCAA enzyme overexpression plasmid were cultivated in lysogeny broth (LB) containing 100 µg/mL ampicillin and 34 µg/mL chloramphenicol at 30ºC. When OD_{600} reached 0.5, the cells were induced with 0.5 mM Isopropyl β-D-1-thiogalactopyranoside. Cells were harvested 4 h post-induction and pelleted by centrifugation. Cell pellets were washed with phosphate buffered

saline and resuspended in sodium phosphate buffer (20 mM, pH7.4) with 0.1 M NaCl. Cells were lysed with a French press via three passes at 1,200 psi and 4ºC. Cell debris was removed by centrifigation and filtration through 0.2-μm low-protein-binding filters. Lysate was then loaded onto a 5-mL Ni Sepharose fast-flow column (GE Healthcare, Piscataway, NJ) connected to a low pressure BioLogic liquid chromatogrphy system (Bio-Rad, Hercules, CA). The column was first washed with buffer containing 20 mM sodium phosphate (pH 7.4), 0.5 M NaCl, and 40 mM imidazole to elmininate nonspecifically bound protein. Elution of the His-tagged enzymes was achieved by increasing the concentration of imidazole from 40 mM to 500 mM in the buffer at a flow rate of 5 mL/min. Fractions containing purified protein of interest were detected on 15% SDS-PAGE gels. These fractions were collected and dialyzed against 20 mM sodium phosphate buffer (pH 7.4) with 0.1 M NaCl using a Slide-A-Lyzer Dialysis Cassette (Thermo Scientific, Asheville, NC, USA) at 4ºC. The proteins were then concentrated using Amicon Ultra-15 Centrifugal Filter Units (EMD Millipore Corporation, Billerica, MA, USA). Lastly, His-tags were removed from the purified proteins using Thrombin Cleavage Kit (Novagen, St. Louis, MO).

Enzymatic activity assays

Purified IlvB, IlvH, IlvC, and IlvD with epitope tags removed were used immediately for enzymatic assays. AHAS was reconstituted by incubating IlvB and IlvH at room temperature for 10 min in solution with 100 mM potassium phosphate buffer (pH 7) and 0.1 mM DTT. IlvB and IlvH mixtures in a molar ratio of 1:0 to 1:100 were tested for reconstitution and enzymatic activity. Protein concentrations were determined by a modified Bradford assay (Zor and Selinger 1996) using bovine serum albumin as the protein concentration standard.

The AHAS, AHAIR, and DHAD activity assays were modified from published methods (Leyval et al. 2003; Lu et al. 2012). The AHAS activity assay is a discontinuous

colorimetric assay. The reaction mixture contained 100 mM potassium phosphate buffer (pH 7.0), 50 mM sodium pyruvate, 100 mM $MgCl_2$, 100 μM thiamine pyrophosphate (TPP), and reconstituted AHAS. Addition of sodium pyruvate initiated the reaction at 30°C. Over the course of the reaction (30 min), 100 μL aliquots of assay mixture were removed every 5 min, and the reaction was terminated by acidification with 10 μL 50% H_2SO_4. The acidified reaction was then incubated at 37°C for 30 min to allow spontaneous decarboxylation of 2-acetolactate to acetoin. Acetoin was quantified by the Voges-Proskauer method (Westerfield et al. 1945) and detected at 535 nm with a Varioskan Flash Plate Reader (Thermo Scientific, Asheville, NC). Different micromolar concentrations of acetoin (3-hydroxy-2-butanone) were used as a standard for determination of the quantity of 2-acetolactate formed.

The AHAIR activity reaction mixture contains 100 mM potassium phosphate buffer (pH 7.0), 10 mM α-acetolactate, 3 mM $MgCl_2$, 0.1 mM NADPH, and purified IlvC. The substrate, α-acetolactate, was chemically synthesized based on a previously published method (Leyval et al. 2003). The addition of α-acetolactate at 30°C initiated the reaction, which was constantly monitored at 340 nm by a spectrophotometer (Agilent 8453 UV-visible Kinetic Mode). Molar extinction coefficient of NADPH (6220 $M^{-1}cm^{-1}$) was used to calculate μmol NADPH oxidized.

The DHAD activity assay indirectly detects the product derivative, α-ketoisovalerate-dinitrophenylhydrazone. The reaction mixture contained 100 mM potassium phosphate buffer (pH 7.0), 5 mM $MgCl_2$, 10 mM DL-α,β-dihydroxyisovalerate, and purified IlvD. Substrate DL-α,β-dihydroxyisovalerate was added to initiate the reaction at 30°C. A 100 μL aliquot of the reaction mixture was removed and the reaction terminated by addition of 12.5 μL trichloroacetic acid (10 % v/v). Aliquots were sampled every 2 min for a total of 20 min. The mixtures were then derivatized with 25 μL saturated 2,4-dinitrophenylhydrazine in 2 M HCl for the formation of α-ketoisovalerate-dinitrophenylhydrazone, which was then detected at

540 nm using a Varioskan Flash Plate Reader. Commercial 3-methyl-2-oxobutanoic acid sodium salt was derivatized and used as a standard for this assay.

Kinetic parameters of AHAS, AHAIR, and DHAD towards substrates and cofactors were determined by measuring the activity of each enzyme at various substrate and cofactor concentrations in the presence of saturating concentrations of all other factors. Pyruvate (from 0.1 mM to 50 mM), 2-acetolactate (from 0.1 mM to 10 mM), and 2,3-dihydroxy-isovalerate (from 0.1 mM to 10 mM) were used for AHAS, AHAIR, and DHAD respectively. FAD from 0.1 μM to 1 μM was used for the AHAS cofactor K_M study and NADPH from 1 μM to 20 μM was used for the AHAIR cofactor K_M study. The K_M and V_{max} values were determined from double-reciprocal plots of kinetic data (Lineweaver-Burk plot). Inhibition assays were conducted by supplementing activity assay mixture with different concentrations of L-valine, L-leucine, or L-isoleucine. The substrate specificity for 2-ketobutyrate as the second substrate (R), was determined by measuring the formation of acetohydroxybutyrate and acetolactate in experiments that contained both pyruvate and 2-ketobutyrate. The results were plotted and fit to Equation 1.

All results discussed in this work were average of triplicate reactions $\pm$ standard deviation unless indicated otherwise. Assay reactions without the addition of enzyme or substrates were conducted separately as controls. Enzyme unit (U) was defined as 1 μmol product formed per min.

RESULTS

Purification of AHAS, AHAIR, and DHAD protein from *R. eutropha*

His-tagged versions of IlvB, IlvH, IlvC, and IlvD were expressed in *E. coli* and purified to homogeneity as described in Materials and Methods. Initial solubility tests indicated that both IlvB and IlvH were present mainly in the insoluble fraction (data not shown), even though they are cytosolic proteins. Attempted purification of IlvB and IlvH

from the soluble fraction only resulted in both proteins precipitating from the buffer solution after elution with imidazole. In order to increase the solubility of the target proteins, nonionic detergents were utilized to dissociate any lipid-protein or protein-protein interactions. Nonionic detergents were chosen over ionic and zwitterionic detergent classes, because these detergents do not denature proteins. Tween 20 or Triton X-100 at final concentrations of 1% (v/v) was added separately before cell disruption by French press. The purification process was carried out as described in Materials and Methods, except that both the binding and elution buffers contained 1% (v/v) detergent. The addition of either Tween 20 or Triton X-100 greatly improved solubility of IlvB and IlvH, and also prevented precipitation after purification (data not shown). The purified IlvB protein solution was bright yellow, which indicated the presence of FAD cofactor bound to the protein. Both IlvC and IlvD are soluble proteins, which were able to be purified without the addition of any detergents. Figure 2 shows an SDS-PAGE analysis of each of the purified proteins, all of which except IlvD, appear homogeneous.

Reconstitution of AHAS holoenzyme from isolated subunits IlvB and IlvH

The purified and His-tag removed catalytic subunit (IlvB) alone was able to catalyze the formation of 2-acetolactate, although its activity was only ~12% of AHAS maximum activity (Table 2). The addition of the regulatory subunit (IlvH) was able to enhance the catalytic activity of AHAS. Table 2 shows the increase in specific activity of AHAS upon addition of increasing molar concentration of regulatory subunit. Saturation point was reached at a 1:5 molar ratio of IlvB and IlvH; therefore, for further studies, AHAS was reconstituted in a 1:5 molar ratio of IlvB and IlvH. The specific activity increase with the addition of IlvH indicated that both subunits have been successfully purified in active and fully reconstitutable forms.

Since the catalytic subunit (IlvB) alone has some enzymatic activity, it was unknown if *R. eutropha* cells could survive in the absence of a functional IlvH. To test this, the *ilvH* gene was deleted from the *R. eutropha* genome. The resulting deletion strain (Re2451) was cultivated in minimal media without any supplementation of branched-chain amino acids, and separately in TSB (tryptic soy broth) rich media. Although the wild type *R. eutropha* strain was able to grow in both media and reach OD_{600} of 3.0 in less than 24 h, Re2451 only grew in TSB media, and the growth rate was slightly reduced (Data not shown). This result indicated that there is only one active AHAS present in *R. eutropha* under the examined growth conditions and the holoenzyme requires its regulatory subunit IlvH.

Kinetic parameters for AHAS, AHAIR, and DHAD

AHAS, AHAIR, and DHAD enzyme activities exhibited a Michaelis-Menten kinetic profile. Using double-reciprocal Lineweaver-Burk kinetic data plots, the maximal rate (V_{max}) and the apparent affinity for substrate and cofactor (K_M) were determined for each enzyme (Online resource 3). The maximum activities of the purified AHAS, AHAIR, and DHAD enzymes are 203 mU/mg, 191 mU/mg, and 6.1 U/mg respectively (Table 3). Compared to activities measured in crude extracts of wild type *R. eutropha*, the purified proteins had greater than 20-fold improvement in activities (Lu et al, 2012).

AHAS has a very weak apparent affinity towards pyruvate (10.5 mM), while AHAIR and DHAD have a slight higher affinity for their corresponding substrates at 6.2 mM and 2.7 mM, respectively (Table 3). In order to determine the apparent affinity of AHAS for its cofactors, FAD, which was tightly bonded to the purified IlvB, was removed. The FAD stripping process involved incubation of purified IlvB in 2% (w/v) activated charcoal in a 1.5 M KCl solution containing potassium phosphate buffer (pH 7.0) for 30 min at 4°C. The charcoal was then removed by centrifugation and filtration. The reconstituted AHAS was colorless in the absence of FAD and had a very high affinity towards FAD (0.42 μM), which

was surprising since mechanistically this enzyme should not involve redox cofactors. TPP is required in the catalysis for the decarboxylation of pyruvate and ligation with the second substrate, whether it be pyruvate or 2-ketobutyrate (Duggleby 2006). The amount of TPP required to reach half-maximum activity cannot be determined, since TPP was co-purified with IlvB and could not be removed *in vitro*. AHAIR requires NADPH to catalyze the substrate isomerization and reduction. The apparent affinity of AHAIR towards NADPH, determined from the cofactor concentration required to support half-saturation of enzymatic activity, was 12.5 μM (Table 3).

R. eutropha AHAS catalyzes the formation of both 2-acetolactate and 2-aceto-2-hydroxybutyrate (Figure 1). The flow of substrates depends on the affinity of AHAS for its substrate, therefore substrate specificity of AHAS was determined over a wide range of substrate concentrations. The specificity constant (R) is related to the ratio of product formation rate in relation to substrate concentration. R for the *R. eutropha* AHAS enzyme was determined to be 140, which indicated that the enzyme is highly biased towards 2-ketobutyrate as the second substrate (Online resource 2). This is also consistent with the low apparent affinity of this enzyme towards pyruvate.

Influence of branched-chain amino acids and keto acids on enzyme activity

Wild type *R. eutropha* experiences a lag in growth when cultivated in increasing concentrations of 2-ketoisovalerate or L-valine (Online resources 4 and 5). At a 2-ketoisovalerate concentration of 0.5% (w/v), the lag phase lasted for more than 24 h (Online resource 4). Valine inhibited the growth even further at a concentration of 1 mM (Online resource 5). Such observations indicated that branched-chain amino acids and their intermediate keto acids could influence the activities of AHAS, AHAIR, or DHAD enzymes via allosteric feedback inhibition. Such inhibition led to growth inhibition because the cells are unable to produce isoleucine, which is essential for cell growth in minimal media.

Table 4 shows the amount of L-valine, L-leucine, and L-isoleucine required for reduction of the specific activities of AHAS, AHAIR, and DHAD by 50%. AHAS, being the first committed step in the BCAA biosynthesis pathway, is very sensitive to valine and isoleucine, but moderately sensitive to leucine. Specific activity of AHAS was reduced to 50% by valine, isoleucine, and leucine, in decreasing order of effectiveness (Table 4). Although AHAS is very sensitive to valine, the inhibition is not complete and the inhibition by all three BCAAs is not accumulative (Figure 3). AHAS activity reduction reached a saturation point at approximately 70% with 10 mM valine. Addition of 5 mM of each valine, leucine, and isoleucine reduced the specific activity by only 56% (Figure 3). Intermediates in the valine biosynthesis pathway, 2,3-dihydroxyisovalerate and 2-ketoisovalerate also showed significant inhibition effects towards AHAS. Specific activity was reduced to 14% and 39% by 10 mM 2,3-dihydroxyisovalerate and 2-ketoisovalerate respectively (Figure 3).

The activities of AHAIR and DHAD were also reduced by valine, leucine, and isoleucine. Valine, leucine, and isoleucine at concentrations of 6.9 mM, 9.4 mM, and 39.2 mM, respectively, were required to reduce AHAIR activity by 50%. DHAD was moderately tolerant to high concentrations of valine and leucine, and only slightly inhibited by isoleucine at 200 mM (Table 4). These inhibitions are very specific to BCAAs, since other amino acids such as threonine and methionine had no effect on the specific activities of these enzymes (Figure 3).

Experimental evolution and site-directed mutations

Experimental evolution, followed by isolation and sequencing of the mutated *ilvBH* genes, was employed to generate mutant strain that is resistant to valine regulation. After 60 days of continuous cultivation on increasing concentrations of valine, mutant strain Re2452 was isolated and its growth rate in the presence of various valine concentrations was determined. The growth rate of *R. eutropha* H16 was reduced by more than 50% when the

valine concentration in minimal media reached 5 mM. At the same concentration of extracellular valine, Re2452 grew normally and had the same growth rate as in the absence of valine. Only an approximate 17-20% reduction of Re2452 growth rate was observed when the valine concentration reached 10-18 mM (Figure 4). This indicates that this evolved mutant strain is capable of tolerating high concentrations of valine, and its AHAS could be catalytically active with concentrations as high as 18 mM (Figure 4). Four mutations (N11S, T34M, T104S, and a frameshift at 133) were detected on the IlvH of Re2452 mutant strain (Online resource 6). Reconstitution of the wild type catalytic subunit and the regulatory subunit of Re2452 yielded an enzyme that has characteristics of the wild type holoenzyme, but is less sensitive to valine. This also implies that the frameshift at position 133 did not affect catalytic activity (Figure 5). The mutant strain has a slight higher tolerance towards valine, in addition to increased tolerance towards leucine and isoleucine (Figure 5).

Asparagine at position 11 is conserved in various valine-sensitive AHAS enzymes, but not in valine-insensitive AHAS. Perhaps other conserved residues could also contribute to valine-sensitivity. An alignment of the amino acid sequences of the small subunits of three valine-sensitive AHASs of *E. coli* and *R. eutropha,* and valine-insensitive AHAS II from *E. coli* was conducted and revealed ten amino acid residues (N11, G14, G21, L22, F23, N29, E31, P38, E58, and Q59) that were found to be present only in valine-sensitive AHASs (Online resource 7). It was hypothesized that the N-terminus of IlvH could be responsible for binding valine (Eoyang and Silverman 1986; Kyselková et al, 2010; Leyval et al, 2003), and therefore these conserved residues were replaced individually with residues found in valine-insensitive AHAS II (N11F, G14E, G21R, L22V, F23V, N29H, E31C, and P38A). The resulting IlvH expression plasmids are listed in Table 1. Each mutated IlvH was purified and reconstituted with wild type IlvB. The reconstituted IlvBH(G21R), IlvBH(L22V), IlvBH(F23V), and IlvBH(E31C) enzymes exhibited no catalytic activity. The other mutations had similar specific activities as the wild type AHAS, except for IlvBH(P34A), which had

approximately 25% reduction in enzymatic activity (Figure 5). The ability to tolerate valine was enhanced in enzymes with N11F, G14E, and N29H mutations (Figure 5). The amount of leucine required to reduce AHAS specific activity by 50% was nearly doubled with these point mutations, although these mutations did not dramatically increase tolerance to isoleucine (Figure 5). These mutations also did not improve AHAS tolerance on valine biosynthesis intermediates 2,3-dihydroxyisovalerate and 2-ketoisovalerate (data not shown), which suggested that the binding site for BCAA is distinctive from the binding site of intermediates and their inhibition mechanisms could differ, or the point mutations did not exclude the binding of intermediates.

DISCUSSION

Many technology platforms are being developed to capture and convert common waste carbon-containing compounds into value-added materials. The Gram-negative, facultatively chemolithoautotrophic *R. eutropha* has been demonstrated as a bioproduction platform for biodegradable plastics, biofuels, and pharmaceutical precursors (Brigham et al. 2013; Brigham et al. 2012; Ishizaki et al. 2001; Lan and Liao 2013). A bottleneck in the production of isobutanol in engineered *R. eutropha* has been shown to be the synthesis of 2-ketoisovalerate, a precursor for the synthesis of branched-chain amino acids and various other valuable products. In this study, enzymes involved in the 2-ketoisovalerate biosynthetic pathway were isolated and characterized from *R. eutropha.*

Although DHAD is the most active enzyme of the pathway (~3,000 mU/mg), the flow of carbon into the 2-ketoisovalerate biosynthesis pathway is controlled by AHAS, which is the first enzyme in the pathway and has the lowest specific activity (~180 mU/mg). Compared to other AHAS enzymes (Chipman et al. 1998; Leyval et al. 2003; McCourt and Duggleby 2006), *R. eutropha* AHAS has a very low apparent affinity towards pyruvate. This observation could be explained by the presence of an excess amount of pyruvate inside the cells, since pyruvate

is a precursor for PHA, the native carbon storage molecule. The low affinity could help balance and control the flow of pyruvate into BCAA biosynthesis pathways. Both AHAIR and DHAD have moderate affinities towards their corresponding substrates, since these substrates are intermediates and are present in non-detectable low concentrations (Table 3).

Intracellular concentrations of valine, leucine, and isoleucine were fairly low (<0.5 mM each) in wild type *R. eutropha*. These concentrations reached 1.5 mM, 1.8 mM, and 1.7 mM, respectively, in engineered *R. eutropha* with *ilvBHC* and *ilvD* overexpressed (Lu et al. 2012). At such intracellular BCAA concentrations, the activities of AHAS and DHAIR in the 2-ketoisovalerate biosynthesis pathway are impacted, which causes the cells to have a low growth rate and 2-ketoisovalerate production (Online Resource 5, Table 4). AHAS experiences the most dramatic impact, since the enzyme's IC_{50} for valine is below the intracellular valine concentration. On the other hand, DHAD activity is most likely not affected since the amount of valine, leucine, or isoleucine required to reduce its activity by 50% is well above 100 mM (Table 4).

R. eutropha AHAS is regulated in a sophisticated, complex manner. As depicted in Online Resource 8, AHAS holoenzyme is hypothesized to be a heterotetramer composed of homodimers of large (IlvB) and small (IlvH) subunits. IlvH is required to reach maximal activity of the enzyme (Table 2) and for feedback inhibition by valine, leucine, isoleucine and pathway intermediates (Table 4, Figure 3). The specific activity of *R. eutropha* AHAS (180 mU/mg) is very low compared to that of *C. glutamicum* (157 mU/mg unpurified AHAS) and *E. coli* (300 mU/mg) (Chipman et al. 1998; Krause et al. 2010; Leyval et al. 2003; McCourt and Duggleby 2006). Since no structure is available for any bacterial AHAS, the relevant structural information was inferred from mutagenesis studies and experimental observations. Cofactor FAD, although not hypothesized to be involved in the enzymatic mechanism (Chipman et al, 2005), was co-purified with IlvB, since the purified IlvB was bright yellow in color. Additionally, the reconstituted apo-AHAS (IlvB and IlvH) has a high apparent affinity

towards FAD (Table 3), which indicates that FAD could play a structural role in the assembly of AHAS holoenzyme.

The binding site of valine, leucine, and isoleucine could be located at the homodimer interface of the IlvH N-terminal domain. The relatively valine-insensitive Re2452 differs from wild type at N11S, T34M, T104S, and a frameshift at 133 of its IlvH subunit. Asparagine (N) hypothesized to be located at the interface of the IlvH dimers, was mutated to serine (S), which is smaller in size. This change in size could be responsible for the binding of valine at the IlvH homodimer interface. Mutation at residue 34 from threonine (T) to methionine (M) could also change the size of the binding pocket, thus further inhibited binding of valine. The frameshift mutation at position 133 could have resulted in a mis-translated C-terminus, or truncated protein. This mutated IlvH, when combined with IlvB, had full catalytic activity and was slightly valine insensitive (Online Resource 6, Figure 5). Therefore, the C-terminal portion of IlvH may not be of importance in AHAS catalytic activity, but could take part in BCAA regulation. Such findings were also supported by previously published results on truncated *E. coli* AHAS. *E. coli* IlvH lacking 35, 48, or 80 amino acid residues from the C terminus is capable of activating AHAS for catalysis (Duggleby 2006; Slutzker et al, 2011). Furthermore, these constructs do not bind valine or respond to BCAA-inhibition (Kaplun et al. 2006; Mendel et al. 2003; Mendel et al. 2001). It is unclear how both the N and C terminus of IlvH interact with BCAAs, although studies hypothesized that the mutant forms of AHAS has a weakened IlvH subunit interaction (Kyselková et al. 2010). Additional potential mutations that might contribute to lack of valine sensitivity may exist, although not generated in this study.

Various single mutations (N11F, G14E, and N29H) on the IlvH N-terminus were also able to decrease BCAA inhibition (Figure 5). Mendel et al. (2001) proposed that the IlvH subunit has an α-β sandwich topology, which is structurally homologous to the regulatory domain of 3-phosphoglycerate dehydrogenase (Chipman and Shaanan 2001; Mendel et al.

2001). An *E. coli* IlvH structural model based on the regulatory domain of 3-phosphoglycerate dehydrogenase revealed that N11 and G14 at opposite ends of the putative domain are involved in valine-binding (Kaplun et al. 2006; Mendel et al. 2001; Petkowski et al. 2007). Studies also showed that N11A, G14D, N29H, and A36V mutations in regulatory subunit of *E. coli* IlvH lead to AHAS with drastically reduced valine sensitivity (Mendel et al. 2003, Mendel et al. 2001), which supports the findings in this study regarding *R. eutropha* IlvH. In the reported studies, *E. coli* IlvH subunit with mutation G14D or N29H do not even bind valine. Interestingly, mutations on IlvH that resulted in tolerance to BCAA did not improve tolerance towards 2,3-dihydroxyisovalerate and 2-ketoisovalerate. This could imply that the binding-site for valine-pathway intermediates is different from BCAA binding-site and/or the binding site mutation excludes BCAAs, but not the intermediates. Such a finding was also reported for *C. glutamicum* AHAS (Krause et al. 2010). The binding of BCAA and pathway intermediates at IlvH was hypothesized to cause a conformational change in the heterotetramer interaction, thus resulting in a less stable complex and reducing the catalytic activity of AHAS (Online Resource 8) (Chipman et al. 1998; Eggeling et al. 1987; Eggeling et al. 1997; McCourt and Duggleby 2006; Vinogradov et al. 2006).

Specificity ratio, R, determined for *R. eutropha* AHAS is 140 and is constant over a wide range of substrate concentrations (Online Resource 2). An R-value higher than 60 indicates remarkably high specificity in favor of 2-ketobutyrate (Chipman et al. 1998). Such a bias towards 2-ketobutyrate is likely due to the relative concentrations of pyruvate and 2-ketobutyrate in *R. eutropha* cells, which implies that the concentration of 2-ketobutyrate is much lower than the pyruvate concentration. In PHA-negative *R. eutropha* strains, intracellular pyruvate concentrations can reach approximately 5.7 mM, since pyruvate is a major intermediate in metabolism and the precursor for PHA biosynthesis (Lu et al. 2012). Ketobutyrate, on the other hand, was non-detectable and kept at low intracellular concentrations to avoid metabolic side-reactions and toxicity. Physical limitations exist for

any enzyme to select one substrate in the presence of a competing substrate that is smaller by a single methyl group. It is unknown what contributes to this unique and highly specific selection in *R. eutropha*. Understanding of the molecular basis behind the *R. eutropha* AHAS R-value could allow prediction of product formation rates in an engineered system.

In order to reduce BCAA-induced AHAS inhibition for improved production of 2-ketoisovalerate, N-terminal single amino acid mutation or C-terminal truncation on IlvH (Figure 5, Online Resource 6 and 7) could be utilized in engineered *R. eutropha*. Reducing the AHAS R-value would also help direct carbon flow towards 2-ketoisovalerate, and consequently valuable products. Previous mutagenesis studies on the *E. coli* AHAS II catalytic subunit revealed a ten-fold reduction in R-value when a tryptophan residue at position 464 was mutated to lysine, glutamine, or tyrosine. It was suggested that the indole ring of tryptophan interacts with the extra methyl group on 2-ketobutyrate and stabilizes it in the active site (Steinmetz et al. 2010). Such site-specific mutations on *R. eutropha* AHAS could also improve selectivity towards biosynthesis of 2-ketoisovalerate.

In the present study, enzymes for the production of 2-ketoisovalerate, an intermediate in BCAA biosynthesis pathway of *R. eutropha*, were overexpressed in *E. coli*, isolated and characterized. The synthesis of BCAA is strongly regulated, especially at the AHAS node, by valine, leucine, isoleucine, and pathway intermediates. In order to engineer *R. eutropha* with increased production of 2-ketoisovalerate, AHAS should be engineered to decrease feedback inhibition by intermediates and product of interest, in addition to present a higher affinity towards pyruvate as the second substrate.

REFERENCES

Bar-Ilan A, Balan V, Tittmann K, Golbik R, Vyazmensky M, Hübner G, Barak Z, Chipman DM (2001) Binding and activation of thiamin diphosphate in acetohydroxyacid synthase. Biochemistry 40(39): 11946–11954

Barak Z, Chipman DM (2012) Allosteric regulation in acetohydroxyacid synthases (AHASs) – different structures and kinetic behavior in isozymes in the same organisms. Arch Biochem Biophys 519(2): 167–174

Barak Z, Chipman DM, Gollop N (1987) Physiological implications of the specificity of acetohydroxy acid synthase isozymes of enteric bacteria. J Bacteriol 169(8): 3750–3756

Bowien B, Kusian B (2002) Genetics and control of CO_2 assimilation in the chemoautotroph *Ralstonia eutropha*. Arch Microbiol 178(2): 85–93

Brigham CJ, Gai CS, Lu J, Speth DR, Worden RM, Sinskey AJ (2013) Engineering *Ralstonia eutropha* for production of isobutanol from CO_2, H_2, and O_2 in Advanced Biofuels and Bioproducts. Springer New York 1065–1090

Brigham CJ, Speth DR, Rha C, Sinskey AJ (2012) Whole-genome microarray and gene deletion studies reveal regulation of the polyhydroxyalkanoate production cycle by the stringent response in *Ralstonia eutropha* H16. Appl Environ Microbiol 78(22): 8033–8044

Brigham CJ, Zhila N, Shishatskaya E, Volova TG, Sinskey AJ (2012) Manipulation of Ralstonia eutropha carbon storage pathways to produce useful bio-based products: reprogramming microbial metabolic pathways in Subcellular Biochemistry Springer Netherlands 64: 343–366

Budde CF, Mahan AE, Lu J, Rha C, Sinskey AJ (2010) Roles of Multiple Acetoacetyl Coenzyme A Reductases in Polyhydroxybutyrate Biosynthesis in *Ralstonia eutropha* H16. J Bacteriol 192(20): 5319–5328

Chipman D, Barak Z, Schloss JV (1998) Biosynthesis of 2-aceto-2-hydroxy acids: acetolactate synthases and acetohydroxyacid synthases. Biochim Biophys Acta BBA - Protein Struct Mol Enzymol 1385(2): 401–419

Chipman DM, Duggleby RG, Tittmann K (2005) Mechanisms of acetohydroxyacid synthases. Curr Opin Chem Biol 9(5): 475–481

Chipman DM, Shaanan B (2001) The ACT domain family. Curr Opin Struct Biol 11(6): 694–700

Chunduru SK, Mrachko GT, Calvo KC (1989) Mechanism of ketol acid reductoisomerase steady-state analysis and metal ion requirement. Biochemistry 28(2): 486–493

Cramm R (2009) Genomic view of energy metabolism in *Ralstonia eutropha* H16. J Mol Microbiol Biotechnol 16(1-2): 38–52

Duggleby RG (2006) Domain Relationships in Thiamine Diphosphate-Dependent Enzymes. Acc Chem Res 39(8): 550–557

Eggeling I, Cordes C, Eggeling L, Sahm H (1987) Regulation of acetohydroxy acid synthase in *Corynebacterium glutamicum* during fermentation of α-ketobutyrate to l-isoleucine. Appl Microbiol Biotechnol 25(4): 346–351

Eggeling L, Morbach S, Sahm H (1997) The fruits of molecular physiology: engineering the l-isoleucine biosynthesis pathway in *Corynebacterium glutamicum*. J Biotechnol 56(3): 167–182

Engel S, Vyazmensky M, Vinogradov M, Berkovich D, Bar-Ilan A, Qimron U, Rosiansky Y, Barak Z, Chipman DM (2004) Role of a conserved arginine in the mechanism of acetohydroxyacid synthase: catalysis of condensation with a specific ketoacid substrate. J Biol Chem 279(23): 24803–24812

Eoyang L, Silverman PM (1986) Role of small subunit (IlvN polypeptide) of acetohydroxyacid synthase I from *Escherichia coli* K-12 in sensitivity of the enzyme to valine inhibition. J Bacteriol 166(3): 901–904

Flint DH, Emptage MH (1988) Dihydroxy acid dehydratase from spinach contains a [2Fe-2S] cluster. J Biol Chem 263(8): 3558–3564

Flint DH, Smyk-Randall E, Tuminello JF, Draczynska-Lusiak B, Brown OR (1993) The inactivation of dihydroxy-acid dehydratase in *Escherichia coli* treated with hyperbaric oxygen occurs because of the destruction of its Fe-S cluster, but the enzyme remains in the cell in a form that can be reactivated. J Biol Chem 268(8): 25547–25552

Gollop N, Damri B, Chipman DM, Barak Z (1990) Physiological implications of the substrate specificities of acetohydroxy acid synthases from varied organisms. J Bacteriol 172(6): 3444–3449

Grousseau E, Lu J, Gorret N, Guillouet SE, Sinskey AJ (2014) Isopropanol production with engineered *Cupriavidus necator* as bioproduction platform. Appl Microbiol Biotechnol 98(9): 4277–4290

Harper AE, Miller RH, Block KP (1984) Branched-Chain Amino Acid Metabolism. Annu Rev Nutr 4(1): 409–454

Ishizaki A, Tanaka K, Taga N (2001) Microbial production of poly-D-3-hydroxybutyrate from CO_2. Appl Microbiol Biotechnol 57(1-2): 6–12

Kaplun A, Vyazmensky M, Zherdev Y, Belenky I, Slutzker A, Mendel S, Barak Z, Chipman DM, Shaanan B (2006) Structure of the regulatory subunit of acetohydroxyacid synthase isozyme III from *Escherichia coli*. J Mol Biol 357(3): 951–963

Kohlmann Y, Pohlmann A, Otto A, Becher D, Cramm R, Lu□tte S, Schwartz E, Hecker M, Friedrich B (2011) Analyses of soluble and membrane proteomes of *Ralstonia eutropha* H16 reveal major changes in the protein complement in adaptation to lithoautotrophy. J Proteome Res 10(6): 2767–2776

Krause FS, Blombach B, Eikmanns BJ (2010) Metabolic engineering of *Corynebacterium glutamicum* for 2-ketoisovalerate production. Appl Environ Microbiol 76(24): 8053–8061

Kyselková M, Janata J, Ságová-Marečková M, Kopecký J (2010) Subunit–subunit interactions are weakened in mutant forms of acetohydroxy acid synthase insensitive to valine inhibition. Arch Microbiol 192(3): 195–200

Lan EI, Liao JC (2013) Microbial synthesis of n-butanol, isobutanol, and other higher alcohols from diverse resources. Bioresour Techno Biorefineries 135(1): 339–349

Leyval D, Uy D, Delaunay S, Goergen JL, Engasser JM (2003) Characterisation of the enzyme activities involved in the valine biosynthetic pathway in a valine-producing strain of *Corynebacterium glutamicum*. J Biotechnol 104(1-3): 241–252

Li H, Liao JC (2014) A Synthetic Anhydrotetracycline-controllable gene expression system in *Ralstonia eutropha* H16. ACS Synth Biol ASAP

Li H, Opgenorth PH, Wernick DG, Rogers S, Wu TY, Higashide W, Malati P, Huo YX, Cho KM, Liao JC (2012) Integrated electromicrobial conversion of CO_2 to higher alcohols. science 335(7067): 1596–1596

Lu J, Brigham CJ, Gai CS, Sinskey AJ (2012) Studies on the production of branched-chain alcohols in engineered *Ralstonia eutropha*. Appl Microbiol Biotechnol 96(1): 283–297

Lu J, Brigham CJ, Rha C, Sinskey AJ (2013) Characterization of an extracellular lipase and its chaperone from *Ralstonia eutropha* H16. Appl Microbiol Biotechnol 97(6): 2443–2454

McCourt JA, Duggleby RG (2006) Acetohydroxyacid synthase and its role in the biosynthetic pathway for branched-chain amino acids. Amino Acids 31(2): 173–210

Mendel S, Elkayam T, Sella C, Vinogradov V, Vyazmensky M, Chipman DM, Barak Z (2001) Acetohydroxyacid synthase: a proposed structure for regulatory subunits supported by evidence from mutagenesis. J Mol Biol 307(1): 465–477

Mendel S, Vinogradov M, Vyazmensky M, Chipman DM, Barak Z (2003) The N-terminal domain of the regulatory subunit is sufficient for complete activation of acetohydroxyacid synthase III from *Escherichia coli*. J Mol Biol 325(2): 275–284

Park JH, Lee SY (2010) Fermentative production of branched chain amino acids: a focus on metabolic engineering. Appl Microbiol Biotechnol 85(3): 491–506

Petkowski JJ, Chruszcz M, Zimmerman MD, Zheng H, Skarina T, Onopriyenko O, Cymborowski MT, Koclega KD, Savchenko A, Edwards A, Minor W (2007) Crystal structures of TM0549 and NE1324--two orthologs of *E. coli* AHAS isozyme III small regulatory subunit. Protein Sci Publ Protein Soc 16(7): 1360–1367

Pohlmann A, Fricke WF, Reinecke F, Kusian B, Liesegang H, Cramm R, Eitinger T, Ewering C, Pötter M, Schwartz E, Strittmatter A, Voss I, Gottschalk G, Steinbüchel A, Friedrich B, Bowien B (2006) Genome sequence of the bioplastic-producing "Knallgas" bacterium *Ralstonia eutropha* H16. Nat Biotechnol 24(10): 1257–1262

Quandt J, Hynes MF (1993) Versatile suicide vectors which allow direct selection for gene replacement in Gram-negative bacteria. Gene 127(1): 15–21

Raberg M, Voigt B, Hecker M, Steinbüchel A (2014) A closer look on the polyhydroxybutyrate-(PHB-) negative phenotype of *Ralstonia eutropha* PHB-4. PloS One 9(5):

Slater KLH (1998) Multiple beta-ketothiolases mediate poly(beta-hydroxyalkanoate) copolymer synthesis in *Ralstonia eutropha*. J Bacteriol 180(8): 1979–87

Sambrook J, Russell DW (2001) Molecular cloning: a laboratory manual. Cold Spring Harbor Laboratory, Cold Spring Harbor, N.Y.

Schomburg D, Stephan D (1995) Ketol-acid reductoisomerase in Springer Berlin Heidelberg. 433–437

Schwartz E, Voigt B, Zühlke D, Pohlmann A, Lenz O, Albrecht D, Schwarze A, Kohlmann Y, Krause C, Hecker M, Friedrich B (2009) A proteomic view of the facultatively chemolithoautotrophic lifestyle of *Ralstonia eutropha* H16. Proteomics 9(22): 5132–5142

Simon R, Priefer U, Pühler A (1983) A broad host range mobilization system for *in vivo* genetic engineering: transposon mutagenesis in gram negative bacteria. Nat Biotechnol 1(9): 784–791

Slutzker A, Vyazmensky M, Chipman DM, Barak Z (2011) Role of the C-terminal domain of the regulatory subunit of AHAS isozyme III: use of random mutagenesis with in vivo reconstitution (REM-ivrs). Biochim Biophys Acta 1814(3): 449–455 doi:10.1016/j.bbapap.2011.01.002

Steinmetz A, Vyazmensky M, Meyer D, Barak ZE, Golbik R, Chipman DM, Tittmann K (2010) Valine 375 and phenylalanine 109 confer affinity and specificity for pyruvate as donor substrate in acetohydroxy acid synthase isozyme II from *Escherichia coli*. Biochemistry 49(25): 5188–5199

Tittmann K, Schröder K, Golbik R, McCourt J, Kaplun A, Duggleby RG, Barak Z, Chipman DM, Hübner G (2004) Electron transfer in acetohydroxy acid synthase as a side reaction of catalysis: implications for the reactivity and partitioning of the carbanion/enamine Form of (α-Hydroxyethyl)thiamin diphosphate in a "nonredox" flavoenzyme. Biochemistry 43(27): 8652–8661

Vinogradov V, Vyazmensky M, Engel S, Belenky I, Kaplun A, Kryukov O, Barak Z, Chipman DM (2006) Acetohydroxyacid synthase isozyme I from *Escherichia coli* has unique catalytic and regulatory properties. Biochim Biophys Acta 1760(3): 356–363

Vollbrecht D, El Nawawy MA, Schlegel HG (1978) Excretion of metabolites by hydrogen bacteria. I. Autotrophic and heterotrophic fermentations. Eur J Appl Microbiol Biotechnol 6: 145-155

Vollbrecht D, Schlegel HG (1978) Excretion of metabolites by hydrogen bacteria. II. Influences of aeration, pH, temperature, and age of cells. Eur J Appl Microbiol Biotechnol 6: 157-166

Vollbrecht D, Schlegel HG (1979) Excretion of metabolites by hydrogen bacteria. III. D(-)-3-hydroxybutanoate. Eur J Appl Microbiol Biotechnol 7: 259-266

Vyazmensky M, Sella C, Barak Z, Chipman DM (1996) Isolation and characterization of subunits of acetohydroxy acid synthase isozyme III and reconstitution of the holoenzyme. Biochemistry 35(32): 10339–10346

Vyazmensky M, Steinmetz A, Meyer D, Golbik R, Barak Z, Tittmann K, Chipman DM (2011) Significant catalytic roles for Glu47 and Gln 110 in all four of the C-C bond-making and -breaking steps of the reactions of acetohydroxyacid synthase II. Biochemistry 50(15): 3250–3260

Vyazmensky M, Zherdev Y, Slutzker A, Belenky I, Kryukov O, Barak Z, Chipman DM (2009) Interactions between large and small subunits of different acetohydroxyacid synthase isozymes of *Escherichia coli*. Biochemistry 48(36): 8731–8737

Westerfield WW (1945) A colorimetric determination of blood acetoin. J Biol Chem 161(1): 495–502

Wilde E (1962) Untersuchungen über wachstum und speicherstoffsynthese von hydroenomonas. Archiv Für Mikrobiologie 43(2): 109-137

York, G.M., Stubbe, J., Sinskey, A.J., 2001. New insight into the role of the PhaP phasin of *Ralstonia eutropha* in promoting synthesis of polyhydroxybutyrate. J Bacteriol 183(7), 2394–2397

Zor T, Selinger Z (1996) Linearization of the Bradford protein assay increases its sensitivity: theoretical and experimental studies. Anal Biochem 236(2): 302–308

FIGURE LEGENDS

Fig. 1

Schematic of the branched-chain amino acid (BCAA) biosynthesis pathway in *R. eutropha*. Pyruvate is the precursor for the production of all three branched-chain amino acids. Via acetohydroxyacid synthase (AHAS), two molecules of pyurvate condense to form 2-acetolactate, a precursor for valine. AHAS can also incorporate 2-ketobutyrate as the second substrate with pyruvate to form 2-aceto-2-hydroxybutyrate for the production of isoleucine. Both 2-acetolactate and 2-aceto-2-hydroxybutyrate are then reduced and isomerized to 2,3-dihydroxyisovalerate and 2,3-dihydroxy-3-methylvalerate respectively by the same enzyme, acetohydroxyacid isomeroreductase (AHAIR). Dihydroxyacid dehydratase (DHAD) converts 2,3-dihydroxyisovalerate and 2,3-dihydroxy-3-methylvalerate to the key intermediate 2-ketoisovalerate and 2-keto-3-methylvalerate accordingly. Transaminase (TA) catalyzes the production of valine from 2-ketoisovalerate and isoleucine from 2-keto-3-methylvalerate. Three other enzymes: isopropylmalate synthase (IPMS), isopropylmalate synthase (IPMD), and isopropylmalate dehydrogenase (IPMDH) sequentially divert 2-ketoisovalerate to leucine production.

Fig. 2

SDS-PAGE gel images of His-tag purified IlvB (A), IlvH (B), IlvC (C), and IlvD (D) after thrombin cleavage. The molecular weight of each protein is 64 kDa, 18 kDa, 36 kDa, and 59 kDa respectively for IlvB, IlvH, IlvC, and IlvD.

Fig. 3

Specific activites of AHAS in the presence of no inhibitors (None), 10 mM L-valine (Val), 5 mM each of valine, leucine, and isoleucine (BCAAs), 10 mM L-threonine (Thr), 10 mM L-

methionine (Met), 10 mM 2,3-dihydroxy-isovalerate (DHIV), and 10 mM 2-ketoisovaleate (KIV). Data present average of three experiments and error bars represent the standard deviation.
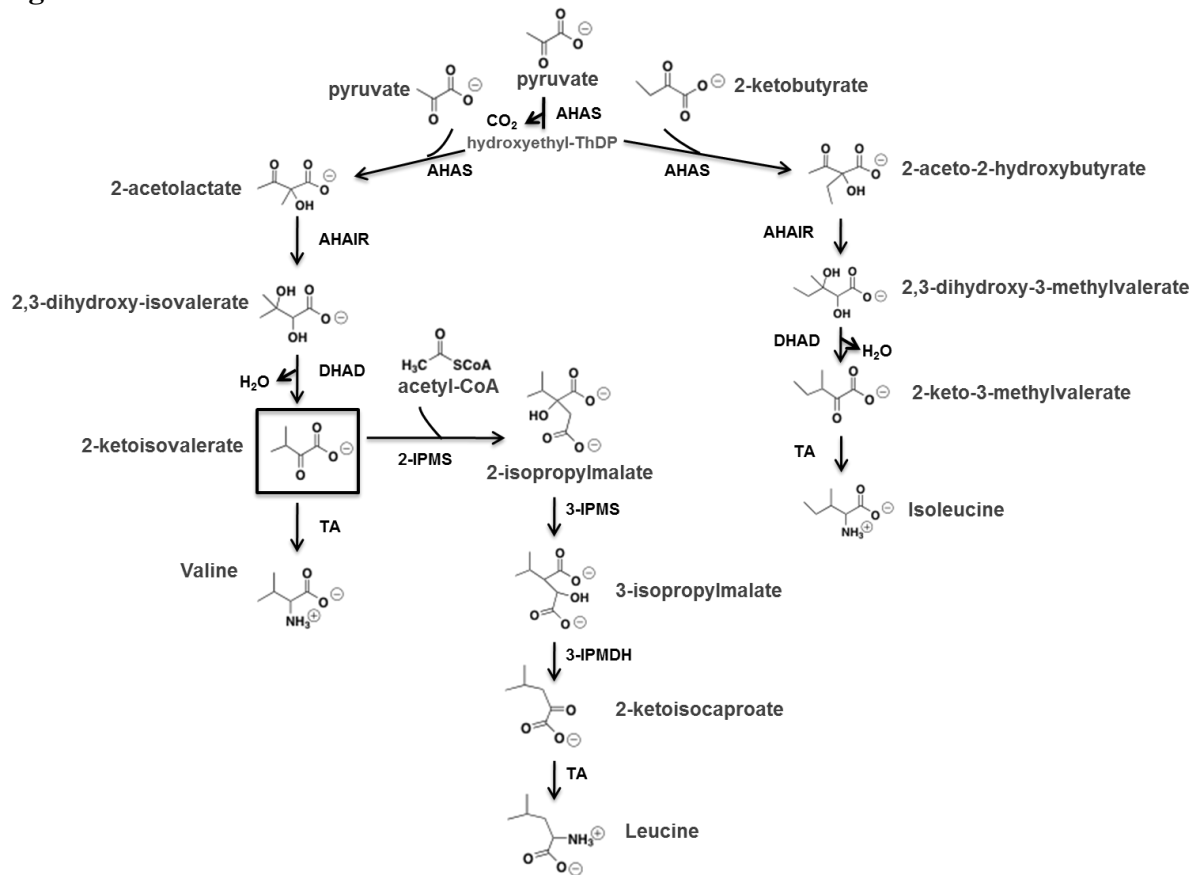
Fig. 4

Growth rate of wild type *R. eutropha* H16 compared to mutant strain Re2452 on L-valine concentrations of 0 mM, 2 mM, 5 mM, 10 mM, 18 mM, and 25 mM. All data points are averages from triplicate cultures and error bars represent the standard deviation.
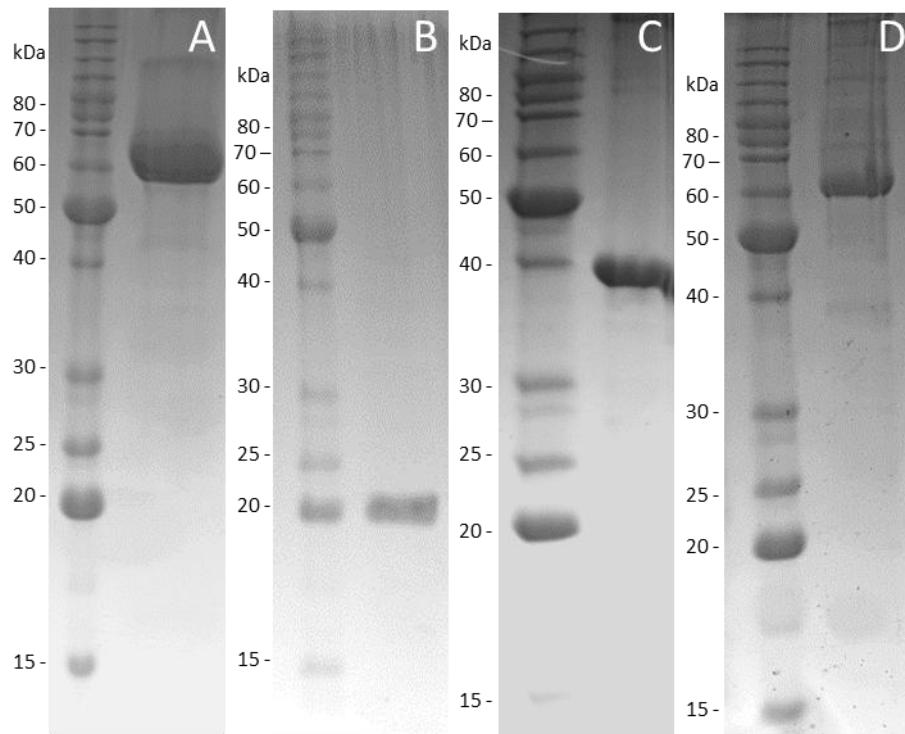
Fig. 5

Influence of L-valine, L-leucine, and L-isoleucine on the specific activities of native IlvB reconstituted with mutated IlvH. Purified wild type IlvB and mutated IlvH proteins were mixed in 1:5 molar ratio. AHAS activity assays were carried out with supplementation of L-valine, L-leucine, and L-isolucine at concentration range of 0.2 to 10 mM separately. IlvB and IlvH with single mutation of G21R, L22V, F23V, and E31C did not have any AHAS enzymatic activity. Values reported here are averages of two experiments.

FIGURES
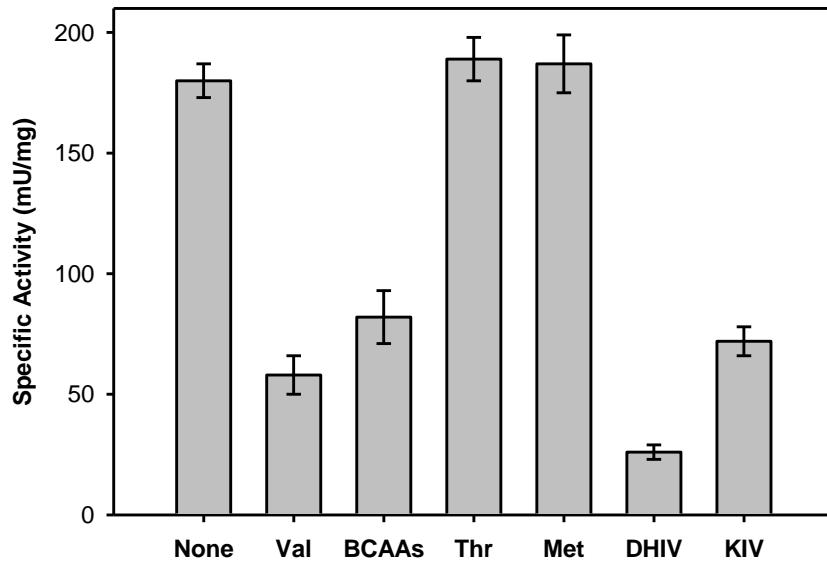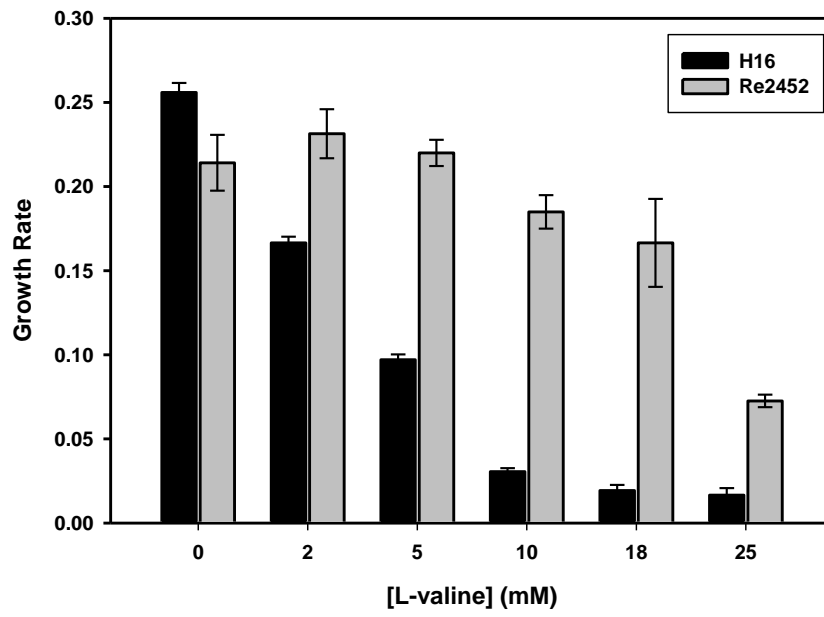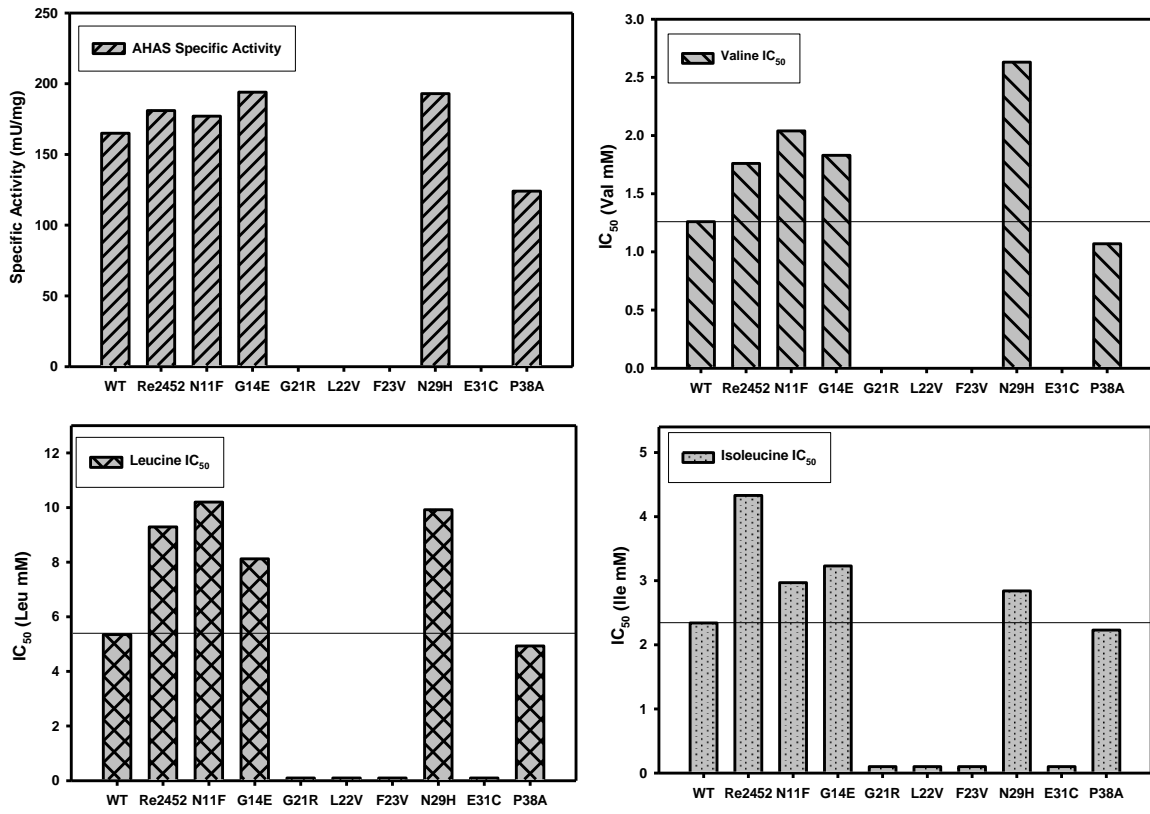
Fig. 1

Fig. 2

Fig. 3

Fig. 4

Fig. 5

TABLES

Table 1

Strains and plasmids used in this work.

Strains or plasmid	Genotype	Reference
Strains		
R. eutropha		
H16	Wild-type, gentamicin resistant (Gen^r)	ATCC17699
Re2451	H16Δ*ilvH* (Gen^r)	This work
Re2452	H16 evolved on L-valine (Gen^r)	This work
E. coli		
DH5α	General cloning strain	Invitrogen
S17-1	Conjugation strain for transfer of plasmids into *R. eutropha*	(Simon *et al.*, 1983)
Tuner(DE3)	Protein expression strain	Novagen
Plasmids		
pJV7	pJQ200Kan with Δ*phaC1* allele inserted into *Bam*HI restriction site, confers kanamycin resistance (Kan^r)	(Budde *et al.*, 2011a)
pJL44	pJV7 with Δ*phaC1* allele removed by *Xba*I and *Sac*I digestion and replace with Δ*ilvH* allele (Kan^r)	This work
pET-15b	Plasmid for inducible and His-tagged protein expression in *E. coli* (Amp^r)	Novagen
pRARE2	Plasmid supplying seven rare *E. coli* tRNAs (Cm^r)	Novagen
pJL13	Plasmid for expression of native IlvB with N-terminal His-tag	This work
pJL14	Plasmid for expression of native IlvH with N-terminal His-tag	This work
pJL15	Plasmid for expression of native IlvC with N-terminal His-tag	This work
pJL16	Plasmid for expression of native IlvD with N-terminal His-tag	This work
pJL45	Plasmid for expression of mutated-IlvH with N-terminal His-tag from strain Re2452	This work
pJL46	Plasmid for expression of native IlvH (N11F) with N-terminal His-tag	This work
pJL47	Plasmid for expression of native IlvH (G14E) with N-terminal His-tag	This work
pJL48	Plasmid for expression of native IlvH (G21R) with N-terminal His-tag	This work
pJL48	Plasmid for expression of native IlvH (L22V) with N-terminal His-tag	This work
pJL50	Plasmid for expression of native IlvH (F23V) with N-terminal His-tag	This work
pJL51	Plasmid for expression of native IlvH (N29H) with N-terminal His-tag	This work

pJL52	Plasmid for expression of native IlvH (E31C) with N-terminal His-tag	This work
pJL53	Plasmid for expression of native IlvH (P38A) with N-terminal His-tag	This work

Table 2

Reconstitution of AHAS holoenzyme from isolated subunits IlvB and IlvH[a].

Ratio of IlvB to IlvH	Specific activity (mU/mg)
1:0	36 ± 5
1:1	130 ± 13
1:5	179 ± 8
1:10	203 ± 41
1:25	194 ± 12
1:50	130 ± 7
1:100	94 ± 11

[a]Purified IlvB and IlvH proteins were mixed in the molar ratio indicated here and incubated at room temperature for 10 min. AHAS activity assay was performed with each of the ratio mixture to determine the rate of acetolactate formation. Specific activity represents nmol acetolactate formed per mg of reconstituted-holoenzyme from its subunits (mU/mg).

Table 3

Specific activity, K_M, and V_{max} values for substrates and cofactors of AHAS, AHAIR, and DHAD[a].

	Specific activity	K_M (substrate)	K_M (cofactor)	V_{max}
AHAS	179 ± 8 mU/mg	10.5 mM (pyruvate)	0.42 µM (FAD)	203 ± 41 mU/mg
AHAIR	288 ± 63 mU/mg	6.2 mM (α-acetolactate)	12.5 µM (NADPH)	191 ± 3 mU/mg
DHAD	3.4 ± 0.3 U/mg	2.7 mM (2,3-dihydroxy-isovalerate)	NA[b]	6.1 ± 0.6 U/mg

[a]K_M, and V_{max} values were determined from the double-reciprocal plot of kinetic data on Lineweaver-Burk plots. Value represents the mean ± standard error on n = 3.

[b]DHAD does not require any cofactor for catalysis.

Table 4

Influence of L-valine, L-leucine, and L-isoleucine on the specific activities of AHAS, AHARI, and DHAD[a].

IC_{50}	Val (mM)	Leu (mM)	Ile (mM)
AHAS	1.3	5.4	2.3
AHARI	6.9	9.4	39.2
DHAD	131	128	NA[b]

[a]Activity assays were carried out with supplementation of each branched-chain amino acid. L-valine, L-leucine, and L-isoleucine concentration ranges of 0.1 to 10 mM, 1 to 10 mM, and 10 to 200 mM were added for the 50% activity reduction determination of AHAS, AHARI, and DHAD respectively.

[b]200 mM of L-isoleucine reduced DHAD activity by less than 5%.